

# Artificial Neural Networks Approach for Earthquake Deformation Determination of Geosynthetic Reinforced Retaining Walls

Tahir Erdem Ozturk <sup>\*1</sup>

Received 24<sup>th</sup> November 2013, Accepted 28<sup>th</sup> December 2013

**Abstract:** Back-to-back Mechanically Stabilized Earth (MSE) walls are commonly used for bridge approach embankments. Artificial Neural Network (ANN) analysis conducted in this study was applied for the first time in literature to estimate the seismic-induced permanent displacements of retaining walls under dynamic loads. For this purpose, a parametric study of seismic response analysis of reinforced soil retaining structures was performed to train the ANN using finite element analysis. The variables used to define wall geometry were reinforcement length, reinforcement spacing, wall height and facing type. The harmonic motion had three different levels of peak ground accelerations, namely 0.2g, 0.4g and 0.6g and had a duration of 6 sec with a frequency of 3 Hz. Although developing an analytical or empirical model is feasible in some simplified situations, most data manufacturing processes are complex and, therefore, models that are less general, more practical and less expensive than the analytical models are of interest. The agreement of the neural network predicted displacements and deformation classification with Finite Element Analyses results were encouraging by the means of correlation since the coefficient values of  $R=0.99$  for ANN regression analysis were achieved.

**Keywords:** Finite element analysis, Artificial neural network, Reinforced soil wall.

## 1. Introduction

According to their economic advantages and superior engineering properties, construction of back to back mechanically stabilized earth (MSE) walls for bridge abutments are becoming more common throughout the world. Displacement based seismic performance studies of these structures have a vital role for the continuity of urban transportation after earthquakes. Although it is known that the seismic performance is related to wall geometry and earthquake characteristics, to gain better insight into mechanisms affecting the behaviour of these structures under dynamic loading conditions several engineering approaches are still being enhanced. The performance of MSE walls under seismic loading can be performed not only with physical testing methods (shaking table, centrifuge, full scale model) but also with analytical and numerical approaches which can be divided into pseudo-static (Monobe-Okabe) methods, displacement (Newmark) methods and finite element methods (FEM).

Finite element analysis is a preferred method because of its time and cost efficiency and holds much promise for simulating the behaviour of reinforced soil retaining structures under dynamic loading conditions. Especially for parametric studies that require large numbers of analysis, the validated FEM technique is preferred instead of time consuming and expensive physical tests. In this study Plaxis v.11.0, a popular FEM software program was used in the analysis of seismic response of reinforced soil walls. Geotechnical applications require advanced constitutive models for the simulation of the nonlinear and time dependent behaviour of soils. The modelling of the soil itself is an important issue; many geotechnical engineering projects involve the modelling of the structures and the interaction between the structures and the soil. Although developing an analytical or empirical model is feasible,

most numerical analysis data manufacturing processes are complex and, therefore, models that are less general, more practical and less expensive than the analytical models are of interest. An important advantage of using Artificial Neural Network (ANN) over regression in process modelling is its capacity in dealing with multiple inputs or responses while each regression model is able to deal with only one response. Another major advantage for developing ANN process models is that they do not depend on simplified assumptions such as linear behaviour or production heuristics. Neural networks possess a number of attractive properties for modelling a complex mechanical behaviour or a system: universal function approximation capability, resistance to noisy or missing data, accommodation of multiple nonlinear variables for unknown interactions, and good generalization capability. ANNs can efficiently be used as a tool for performing tasks such as function approximation (regression) and classification.

In the literature starting from 1990s, ANNs have been used productively for solving major particular problems in geotechnical engineering. Classical constitutive modelling is unable to imitate the situation of geomaterials because of formulation complexity, and undue empirical options. According to this, many researchers [2-21-22]; claimed that constitutive modelling is based on the elasticity and plasticity theoretician, and suggest neural networks as a dependable and practical disjunctive to modelling the constitutive monotonic and hysteretic behaviour of geomaterials. To prevent damage caused by failure of soils as in liquefaction, there are different types of ANNs which take into account many applications in geotechnical engineering which include retaining walls ([6-12], dams [10], blasting [14], geo-environmental engineering [15], and tunnels and underground openings [4-18]. Ural and Saka [17]; Young-Su and Byung-Tak [19] also carried out studies to investigate the applicability of ANNs for predicting liquefaction.

<sup>1</sup>Boğaziçi University, Turkey, \* Email: erdemtahir@hotmail.com

Goh et al. [6] developed a neural network model to provide initial estimates of maximum wall deflections for braced excavations in soft clay. The neural network was used to synthesize data derived from finite element studies on braced excavations in clay. The input parameters used in the model were the excavation width, soil thickness/excavation width ratio, wall stiffness, height of excavation, soil undrained shear strength, undrained soil modulus/shear strength ratio and soil unit weight. The maximum wall deflection was the only output.

**Table 1.** Comparison of neural network prediction and field measurements [6]

Case History	Measured wall deflection (mm)	Predicted wall deflection (mm)
Laveder (Singapore)	32	31
Laveder (Singapore)	36	28
Telecom (Singapore)	56-84	65
Vaterland 3	76	76
NGI (1962)	114-140	107
San Francisco	20-60	59
Mana (1977)	72-150	122

## 2. Theory and Methodology

### 2.1. Artificial Neural Networks

Zurada [23] and Fausett [5] explained that ANNs consist of a number of artificial neurons known as 'processing elements' (PEs), 'nodes' or 'units'. For multilayer perceptrons (MLPs), which are the most commonly used ANNs in Geotechnical engineering, processing elements are situated as an input layer, an output layer and one or more intermediate layers called hidden layers (Fig. 1). The dissemination of data in MLPs begins at the input layer where the input data are submitted. During the process each input is weighted, summed and elapsed through a transfer function to make the nodal output. If the network cannot find a set of weights that perform the input-output mapping, it will be still regulating its weights on presentation of a set of training. This process is called 'learning' or 'training'.

Since the training set of a model has been finished effectively it must be validated. The aim of validation is to check the capacity of the model to generalize the limits set by the training data. If this type of procedure is appropriate, the model is considered robust enough to be generalized.

The coefficient of correlation,  $r$ , the root mean squared error, RMSE, and the mean absolute error, MAE, are the main criteria that are often used to evaluate the prediction performance of ANN models. The coefficient of correlation, a value defined between 0.0 and 1.0, is a measure that is used to determine the relative correlation and the goodness-of-fit between the predicted and observed data.

The objective of the linear regression model is to find the unknown function  $f$ , which relates the input variable  $x$  to the output variable  $y$ . The function  $f$  can be obtained by changing the slope  $\tan\phi$  and intercept  $\beta$  of the straight line in Fig. 2.a, so that the error between the actual outputs and outputs of the straight line is minimized. The

same principle is also used in ANN models. ANNs can form the simple linear regression model by having one input, one output, no hidden layer nodes and a linear transfer function (Fig. 2.b). The connection weight  $w$  in the ANN model is equivalent to the slope  $\tan\phi$  and the threshold  $\theta$  is equivalent to the intercept  $\beta$ , in the ANN linear regression model.

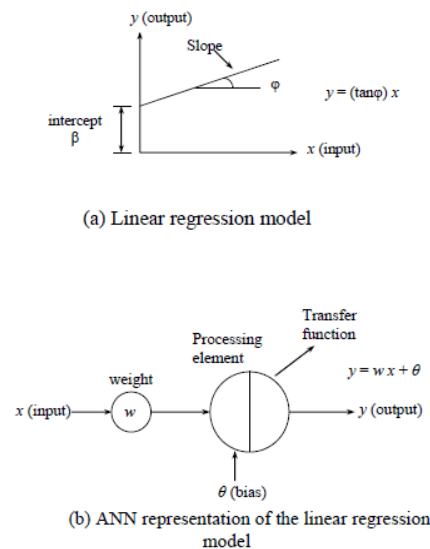


**Fig. 2.** Linear regression versus ANN models [5].

It is known from previous studies [7] that the peak ground acceleration and the wall displacements are not linearly related. When there are non-linear problems, ANNs can deal with these by changing the transfer function or network structure, and the type of non-linearity can be replaced by changing the number of hidden layers and the number of nodes in each layer.

### 2.2. Strong Ground Motion and Intensity Measures

In estimating strong-motion characteristics for seismic design, there is a need to define the parameters that reflect the destructive potential of the motion. Providing quantitative estimates of expected levels of seismic ground-motion requires characterizing the complex nature of strong-motion accelerograms by using simple parameters and the development of predictive relationships for these parameters.

The main elements of earthquake engineering field and structural dynamics are ground motion time history records of acceleration, velocity and displacement. Among the information included in time history record, amplitude, frequency content and duration characteristics of the strong ground motion are the most crucial ones for engineering purposes [11]. Several ground motion parameters have been defined in the literature and are listed as follows; peak ground acceleration (PGA), peak ground velocity (PGV), effective peak acceleration (EPA), arias intensity (AI), cumulative absolute velocity (CAV), acceleration spectrum

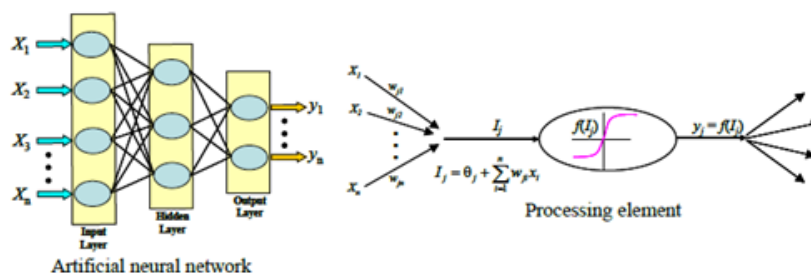


**Fig. 1.** Typical structure and operation of ANNs [23].

intensity (ASI), and velocity spectrum intensity (VSI).

In this study SeismoSignal, software used to process strong motion data, was utilized to determine all these IM's from acceleration time history for three different harmonic motions that are varied with respect to PGA values. This software comprises an efficient and simple way to process strong-motion data, featuring a user-friendly visual interface and the capability of deriving a number of strong-motion parameters.

Uang and Bertero [16] examined the adequacy of the parameters that have been used to identify the damage potential of an earthquake and reported that the destructiveness of a ground motion record at the foundation of a structure relies on the intensity, frequency content, duration and the dynamic characteristics of the structure. They reached the conclusion that the most dependable parameter for measuring the damage potential is earthquake energy input.

### 3. CALCULATIONS

#### 3.1. Numerical Model with FEM

In this study, Plaxis, an extensively used finite element program was utilized for the numerical analysis. Two dimensional (2-D) plane strain analysis was performed during the study.

As can be seen from Fig. 3, the boundary conditions were identified as fixities; at the bottom boundary total fixity was identified which means both horizontal ( $u_x$ ) and vertical ( $u_y$ ) are zero. Below the wall level at the right and left boundaries of the basement only horizontal fixities were assigned.

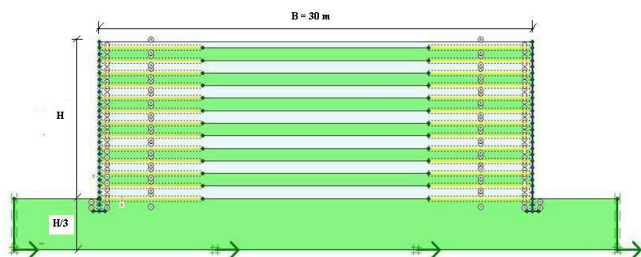


Fig. 3. The geometry of the back to back wall model

The absorbent boundaries were used in dynamic calculations to account for the fact that in reality soil is semi-infinite medium. Although these boundaries also affect the wall displacements, without these boundaries the waves would be reflected from the model boundaries, returning into the model and disturbing the results. To avoid these spurious results reflection absorbent boundaries were specified at the bottom right and left side boundary. In order to minimize absorbent boundary effects on wall displacements, the back to back retaining wall was used as the most adaptable and realistic design. The geometry of these FEM models was defined as in all models the width (B) was fixed at 30 m. and the height of the wall (H) got values between 5m and 10m. Below the ground level one concrete panel or one modular block was embedded as a foundation.

The linear elastic perfectly-plastic Mohr-Coulomb Model (MCM) model was used to define the backfill soil. The model involves five input parameters, E and  $\nu$  for soil elasticity;  $\phi$  and c for soil plasticity and  $\psi$  as an angle of dilatancy and the values were assigned as stated in Table 2.

Table 2. Material properties of soil

Material Model	Unit Weight ( $\gamma_{dry}$ )	Elasticity Modulus (E)	Poisson Ratio ( $\nu$ )	Cohesion (c)	Internal Friction Angle ( $\phi$ )	Dilatancy Angle ( $\psi$ )
Mohr-Coulomb	18 kN/m <sup>3</sup>	30000 kN/m <sup>2</sup>	0.3	5 kN/m <sup>2</sup>	35°	0°

The reinforcing elements used to define geotextiles could only sustain tensile forces and have no bending stiffness. For modelling elastoplastic behaviour, the maximum tension force in any direction is bound by  $N_p$ . For geotextile reinforcements  $EA=4,000$  kN/m was chosen for elastic axial stiffness and  $NP=400$  kN/m for 10% strain condition.

In our parametric analysis, modular block facing and precast concrete panel were used as facing elements. The modular block facing elements were modelled as 0.5 m in width and 0.25 m in height and linear elastic material model was selected to define the material with properties; unit weight ( $\square_{dry}$ ) was 21 kN/m<sup>3</sup>, elastic modulus (E) was  $4.4 \times 10^6$  kN/m<sup>2</sup> and Poisson ratio ( $\nu$ ) was 0.17. Precast facing panels were modelled using plates of 0.60 m of width and height and 0.20 m of thickness. The material properties were defined as 23.5 kN/m<sup>3</sup> for unit weight,  $25 \times 10^6$  kN/m<sup>2</sup> for elastic modulus, 0.20 for Poisson ratio and 28 MPa for 28-day compressive strength. Based on these properties, the axial stiffness EA was calculated as 5,000,000 kN/m. Bending stiffness EI was found as 16,660 kNm<sup>2</sup>/m and finally, for one meter height, the weight of the panels was found to be equal to 4.7 kN/m.

The connection between facing panels is modelled by some researchers by simple hinges and the compressibility that develops between them due to the presence of pads is neglected. Since deformations are the main outcome of this study, instead of hinges rubber bearing pads were modeled using the same type of elements that were used for the facing panels.

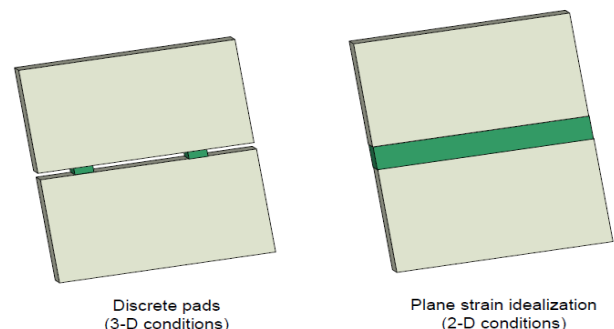


Fig. 4. Modeling of discrete bearing pads in plane strain analysis.

Taking into account the cross sectional area of the rubber pad, which is 0.0085 m<sup>2</sup>, the axial stiffness is equal to 400 kN/m. However, this refers to one pad with dimensions 100 mm \* 85 mm \* 60 mm. In plane strain analysis illustrated in Fig. 4, the pad was replaced by a plate whose equivalent axial stiffness was calculated as 533.3 kN/m. Knowing the thickness of the pads ( $d = 0.085$  m), the bending stiffness per linear meter was found equal to 0.321 kNm<sup>2</sup>/m. Note that pads are assumed to be weightless and to have a very high Poisson's ratio of 0.495.

In the present finite element model, elements were placed between the precast concrete panel and the backfill soil interface. The interfaces were also placed between all modular block elements. The strength reduction factor value was chosen as 0.7 between backfill soil and precast concrete panel and between modular blocks.

The Finite Element Model was subjected to a base excitation, which is a variable amplitude harmonic motion. The prescribed displacement feature of the program at the base of the wall was

employed to assign the constant frequency cyclic load. The cyclic load was applied at equal time intervals of 0.05 s and its variation with time is shown in Fig. 5. This accelerogram has been accepted as a good representation of commonly encountered accelerograms [3]. The peak amplitude of the input acceleration was selected as 0.2, 0.4 and 0.6 g. A frequency of 3 Hz was selected to represent a typical predominant frequency of medium to high frequency content earthquake.

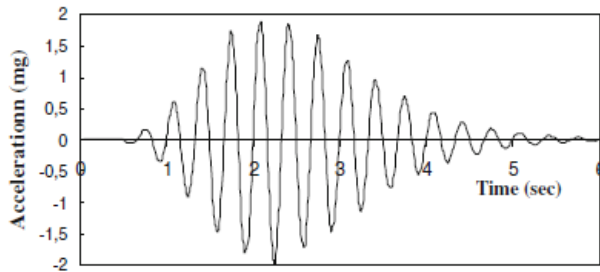


Fig. 5. Base harmonic acceleration history used as cyclic load in the analysis (apeak=0.2g).

### 3.2. Validation Analysis of Numerical Model

In order to validate the finite element modeling technique under earthquake loading conditions, the results of a shaking table test reported by Ling et al. [13] were used and the results were compared and reported by Guler et al. [7].

To check the accuracy of the Finite Element Model (FEM) used in this study, results of a 1-g shaking test reported by Anastopoulos et al. [1] were modeled using the same Finite Element modeling technique.

Anastopoulos et al. [1] performed tests on back to back retaining walls. The configuration details of model setup are shown in Fig. 6. Two different steel wire meshes were used in order to simulate flexible and stiff reinforcements. Plane strain idealization of discrete reinforcement elements was used in order to transform 3-D conditions of physical test to a 2-D finite element model according to the study of Zevgolis [20]. After this adjustment, the elastic axial stiffness parameters which were required for numerical analysis were calculated as  $EA = 400 \text{ kN/m}$  for stiff and  $40 \text{ kN/m}$  for flexible reinforcement.

The facing panels were made of  $t=2 \text{ mm}$  Plexiglas strips ( $E = 3 \text{ GPa}$ ), and were connected to each other through a customized connection using a "shear key" configuration to block relative horizontal displacements between consecutive panels but allowing differential rotation (as in reality). Based on these properties, the axial stiffness  $EA$  was calculated as  $6,000 \text{ kN/m}$ . Bending stiffness  $EI$  was found as  $2 \times 10^{-3} \text{ kNm}^2/\text{m}$ . Poisson's ratio and unit weight of Plexiglas strip facing were assigned as 0.37 and  $0.0234 \text{ kN/m/m}$  respectively for numerical analysis. The backfill consisted of dry "longstone" sand, a very fine and uniform quartz sand industrially produced with adequate quality control. Test model was constructed with  $D_r = 44\%$  to represent the loose state (Table 3).

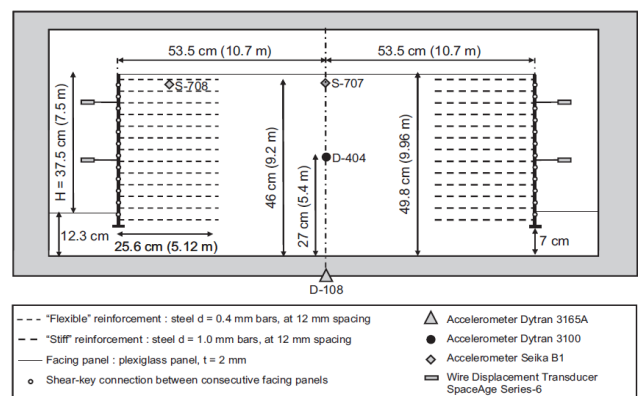


Fig. 6. Shaking table model setup showing geometry and instrumentation. [1]

Table 3. Longstone sand index properties of validation model. [1]

Specific gravity ( $G_s$ )	2.64
Maximum void ratio ( $e_{max}$ )	0.995
Minimum void ratio ( $e_{min}$ )	0.614
Median diameter ( $D_{50}$ ) (mm)	0.15
Uniformity coefficient, ( $C_u$ )	1.42
Unit weight ( $\text{kN/m}^3$ )	18
Friction Angle ( $\phi$ )	$36^\circ$
Relative Density ( $D_r$ )	44%
Poisson Ratio ( $\nu$ )	0.3
Dilation Angle ( $\psi$ )	$6^\circ$

The model was subjected to an "extreme seismic shaking 60-cycle cos sweep" of dominant period  $T_0=0.5 \text{ s}$  and  $PGA= 1.0 \text{ g}$  (Fig. 7).

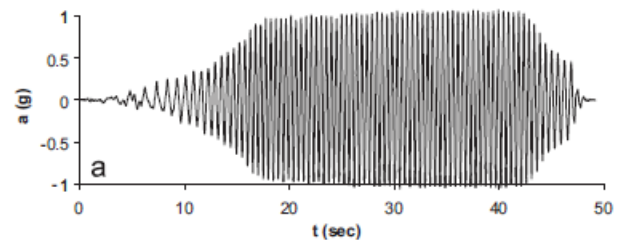


Fig. 7. 60-cycle "extreme shaking" synthetic excitation [1].

Although not realistic (both in terms of retained soil density and shaking intensity), this test was conducted to derive deeper insights on the ultimate capacity of reinforced soil walls.

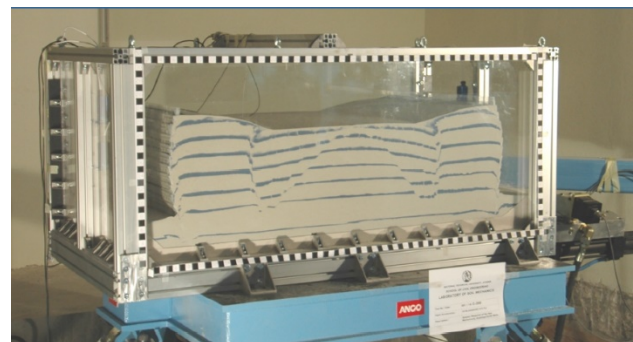


Fig.8. Shaking table test results after harmonic motion. (60-cycle "cos sweep" of dominant period  $T_0=0.5 \text{ s}$  and  $PGA= 1.0 \text{ g}$ ) [1].



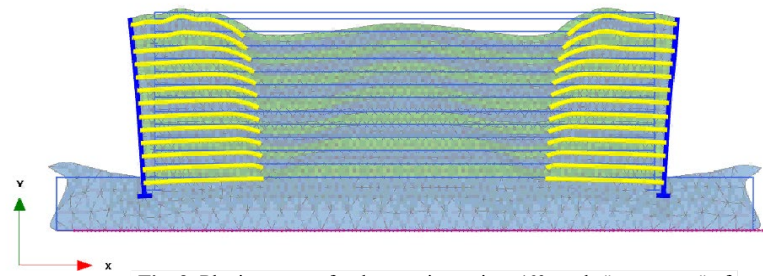


Fig. 9. Plaxis output after harmonic motion. (60-cycle "cos sweep" of dominant period  $T_0=0.5$  s and  $PGA= 1.0$  g).

Fig. 8 shows the final position of the wall after 60-cycle "cos sweep" seismic excitation which has a period  $T_0=0.5$  s and  $PGA=1g$ . Fig. 9. shows the Plaxis models final deformation position.

The order of shaking events started with smaller intensity records, followed by the larger ones, and completed with multi-cycle artificial motions: the two 30-cycle so-called "cos sweeps" of  $PGA=0.5$  g and  $T_0=0.4$  or  $0.8$  s.

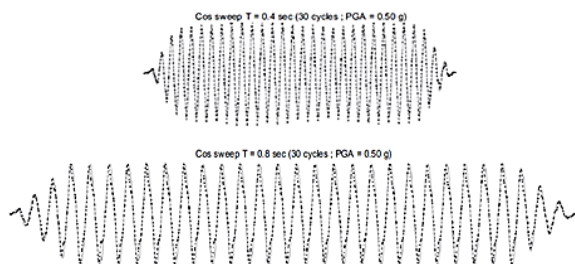


Fig. 10. Multi-cycle accelerograms used as seismic excitations [1].

The results of the numerical analyses are summarized in Fig. 11 and Fig. 12. The results of FEM model are compared directly with shaking table test results to serve as validation of the numerical analysis and of the Mohr Coulomb model.

As depicted in Fig. 11 and Fig. 12 the numerical prediction (analysis of shaking table model) compares well with the results of the shaking table tests for the two artificial 30-cycle cos-sweeps. The numerical analysis underestimates the cyclic component of the horizontal (lateral) wall displacement, but the examined herein (reinforcement stiffness and dominant period of residual displacement).

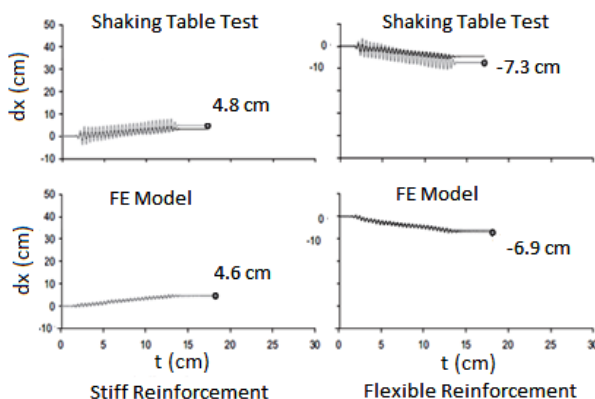


Fig. 11. Wall displacement time histories for the multi-cycle seismic excitation of  $T=0.4$  s

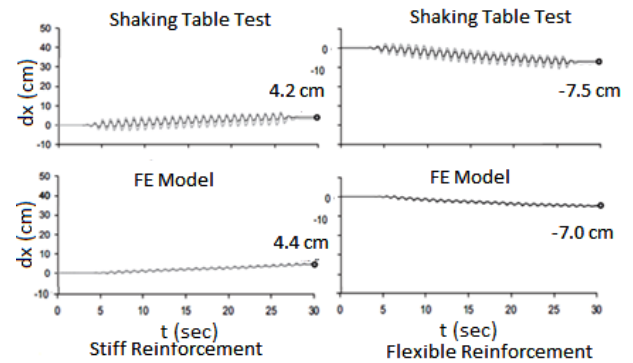


Fig.12. Wall displacement time histories for the multicyle seismic excitation of  $T=0.8$  s

### 3.3. ANN Analysis

In this study, twelve input and one output parameters were used in order to predict the permanent displacement of back to back retaining walls. Five of them were about wall geometry illustrated in Fig. 13 as; wall height ( $H$ ) varied between 5m and 10m, reinforcement length ( $L$ ), length over height ratio ( $L/H$ ) changed between 0.5 and 2, vertical spacing of reinforcement ( $S_v$ ) varied between 0.2m and 0.8m, facing type (modular block and precast concrete panel).

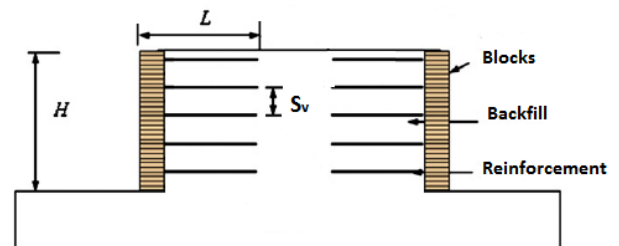


Fig. 13. Back to back retaining wall geometry.

The other seven parameters were about intensity measures of dynamic loading as  $PGA$  ( $m/s^2$ ),  $PGV$  ( $m/s$ ),  $EPA$  ( $m/s^2$ ),  $AI$  ( $m/s$ ),  $CAV$  ( $m/s$ ),  $ASI$  ( $m/s$ ),  $VSI$  ( $m$ ). The program Seismosignal was used to obtain the intensity measure results for a given acceleration time history. Table 4. gives the results of three harmonic ground motion analyses.

Table 4. Seismosignal results of harmonic motion.

Harmonic Ground Motion	PGA ( $m/s^2$ )	PGV ( $m/s$ )	EPA ( $m/s^2$ )	AI ( $m/s$ )	CAV ( $m/s$ )	ASI ( $m/s$ )	VSI ( $m$ )
0.2g	1,977	0,096	1,961	0,5	2,826	2,014	0,317
0.4g	3,999	0,196	3,903	2,151	5,962	4,098	0,644
0.6g	5,93	0,288	5,882	4,505	8,48	6,041	0,95

ANN was initially trained using a set of experimental data obtained from the computer simulations of FE models of the back to back wall and this set of data was called training data. Design of ANN

architecture consists of determining the number of layers, the number of neurons in each layer, activation functions of the neurons and the learning algorithm for the network. The most common ANN architecture is a multi-layer feed-forward structure also known as a multilayer perceptron (MLP) trained by Back-Propagation (BP) algorithm [9]. There are three different types of layers in a MLP: an input layer representing the input design variables, an output layer representing the response, and a number of hidden layers that perform the mapping of the input data before they enter the output layer. (Fig. 14)

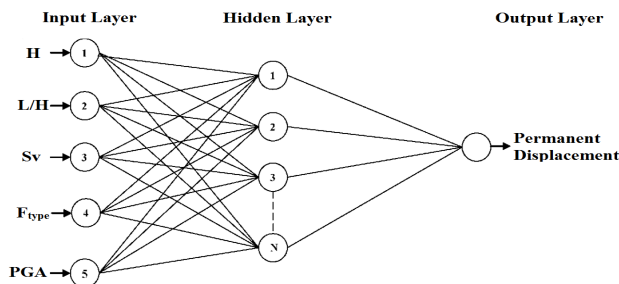


Fig. 14. Multi-layer perceptron (MLP) with three layers.

Other than the training data, validation data were used during the learning process. The learning halts when the error of the validation data falls below a threshold value or when a maximum number of iterations (epochs) is reached. Finally, the performance of the network was estimated using independent test data that had not been used in the learning process. The mean square error (MSE) is generally used for calculating the error. For this study, the Levenberg-Marquardt (LM) algorithm was adopted for its efficiency in training MLP. The details of the back propagation (BP) algorithm can be found in the literature [8].

## 4. RESULTS

### 4.1. Finite Element Analysis Results

Fig. 15 shows deformed models lateral displacement  $|u_x|$  after seismic loading by the means of shadings. Color scale on the right side of deformed model shows the displacement distributions of all systems.

Walls with modular block facing and precast concrete panel facing have different displacement increments behaviour as can be seen from Fig. 16 and Fig. 17. Also it was obtained from figures that in both facing types the permanent displacements increased nonlinearly with increasing PGA values. It was observed that this

increase was more obvious at higher walls for example for a 9 meter wall the permanent displacements were 17, 28 and 32 cm for 0.2, 0.4 and 0.6 g PGAs respectively. As an example, for a 5 meter wall the permanent displacement values did not vary so much with increasing PGA. This on the other hand shows that the relation between permanent displacements and wall height is also non-linear.

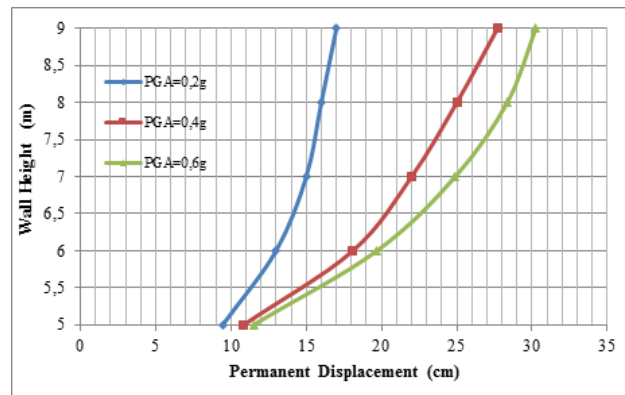


Fig. 16. Permanent displacement according to wall height ( $L/H = 0.7$ ,  $S_v = 40$ cm, modular block facing).

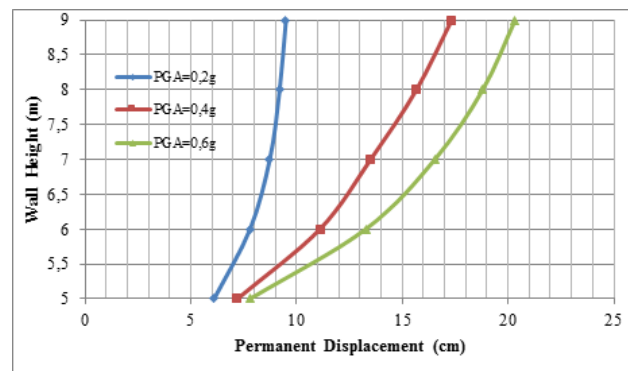


Fig.17. Permanent displacement according to wall height ( $L/H = 0.7$ ,  $S_v = 40$ cm, precast concrete panel facing).

Relative displacement  $\delta_r$  is the ratio of maximum displacement to wall height. Fig.18 shows the variation of  $\delta_r$  values for  $L/H$  ratios for a wall model example where  $S_v = 0.4$ m and  $H = 7$ m obtained from FEM analysis. It can be observed that the relative displacements increased nonlinearly with increasing PGA and the differentiation was more obvious between  $L/H$  ratios of 0.7 and 1. Especially for a PGA of 0.2g it is also clearly seen that the

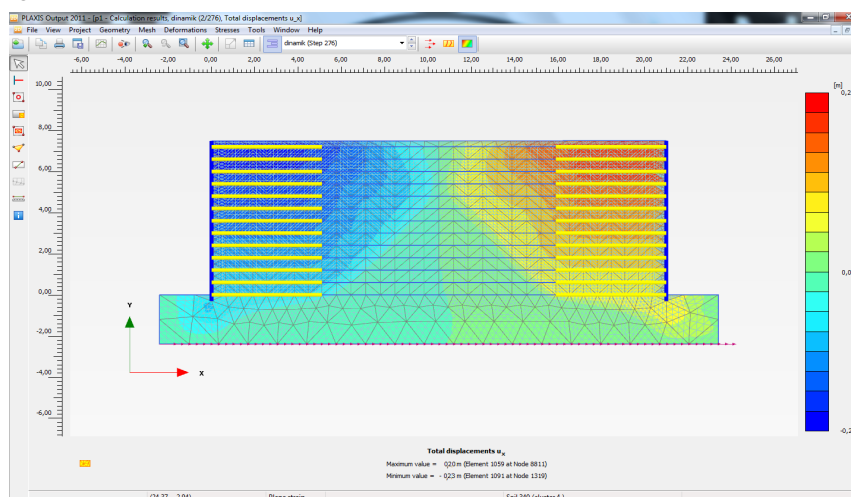


Fig. 15. Deformed mesh after seismic loading (PGA= 0.2g).

relationship between relative displacement and L/H ratio is also non-linear.

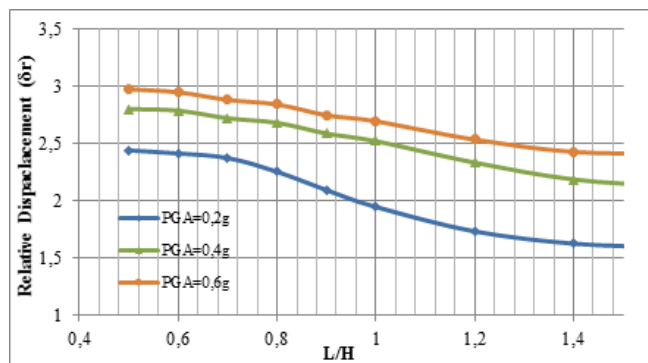


Fig. 18. Relative displacement factors according to L/H. (Sv=40 cm, H=7m)

As can be seen in Fig. 19 displacement values normalized by height are increased with increasing vertical spacing between reinforcements.

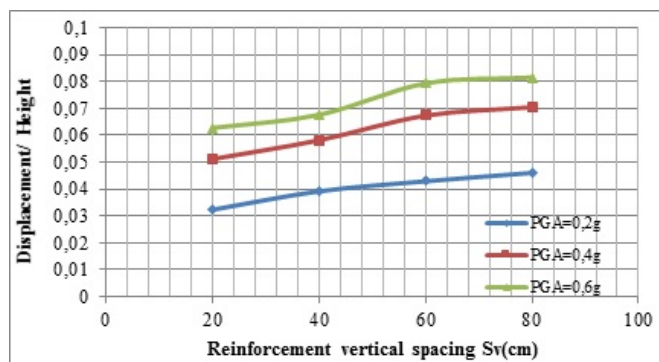


Fig. 19. Displacement / Height according to vertical spacing Sv. (L/H=0.7 H=7 m).

#### 4.2. ANN Regression Analysis Result

Squared Error (MSE) is performance metric adopted to determine the network performance, while regressions; R is used to measure the correlation between outputs and targets. The fitting curve between targets with inputs is shown in Fig.20 and the best validation performance is approached at epoch 10.

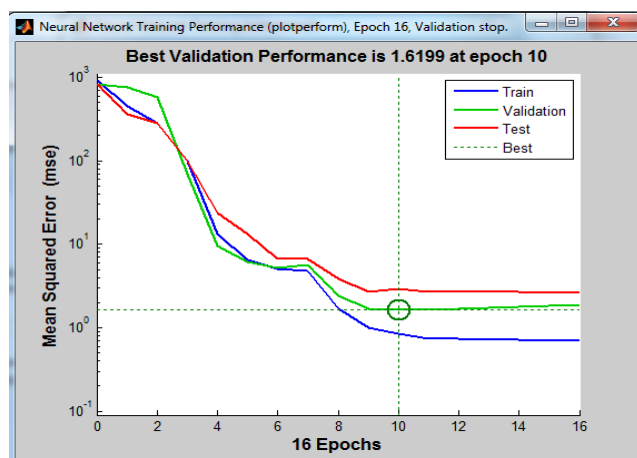


Fig. 20. Validation performance.

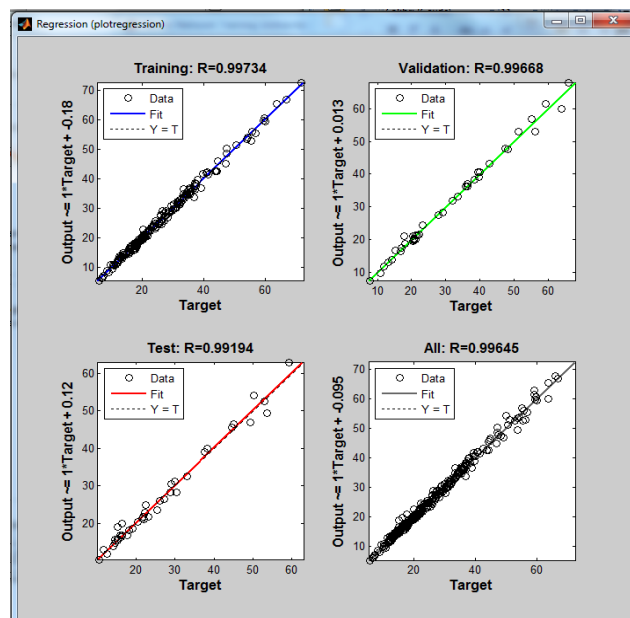


Fig. 21. Fitting curve between targets with inputs.

The neural network is trained and validated using the first batch of 110 learning points and the performance is evaluated using 83 test points. The performance of the ANN regression model for the first 83 learning points using 10 neurons in the hidden layer can be seen in Fig. 21. Even for a relatively low number of learning points, ANN regression performs well on the test data. Totally 276 data are distributed between training, validating and testing in different percentages. Despite distribution of the data in various proportions, no significant change about R has been seen in Table 5.

Table 5. Results for MSE and regression for Different data distribution.

	Number of Samples	MSE	R		Number of Samples	MSE	R
Training	110	0,8412	0,9972	Training	220	17,781	0,9951
Validating	83	60,033	0,9871	Validating	28	22,581	0,9932
Testing	83	35,156	0,9902	Testing	28	22,096	0,9921

The same geometric input with each intensity measures gives high coefficients of correlation for testing data as seen in Table 6. It is assumed that this result was obtained because a harmonic motion was used in this study.

Table 6. Search for each IM input features.

Number of Features	R (%)	Intensity Measures
1	99.37	PGA
2	98.32	PGV
3	99.24	EPA
4	98.84	AI
5	98.75	CAV
6	99.23	ASI
7	99.42	VSI

The agreement of the neural network predicted displacements and FEA results were encouraging, as shown in Table 7.

Table 7. Comparison of neural network predictions and FEA results.

H (m)	S <sub>v</sub> (m)	L/H	Facing type	PGA	Measured displacement (cm)	Predicted Displacement (cm)
5	0,4	1,4	Modular Block	0,6 g	18,2	18.12
6	0,2	0,5	Modular Block	0,4 g	31,09	29.52
6	0,4	1,2	Modular Block	0,4 g	27,1	26.38
7	0,6	1	Modular Block	0,2 g	23,7	23.25
7	0,8	0,7	Concrete Panel	0,6 g	41	39.8
8	0,2	0,7	Modular Block	0,2 g	24,8	25.6
9	0,4	1	Concrete Panel	0,4 g	32	32.7

## 5. CONCLUSION

In the numerical analysis part of the study permanent displacements of back to back reinforced segmental retaining walls under earthquake loading condition were calculated with the finite elements program Plaxis. Three harmonic motions which have PGA values 0.2g, 0.4g and 0.6g respectively with a frequency of 3 Hz were performed.

The investigated parameters such as height of the wall, type of facing (modular block and concrete panel), reinforcement length and spacing of reinforcement led to the following results. The permanent displacement increased with the height of the wall. Permanent displacements of modular block facing walls were more than precast concrete panel facing. Increasing reinforcement length decreased the permanent displacements of wall facing and maximum tensile stress on reinforcement. Decreased reinforcement vertical spacing ( $S_v$ ) caused a reduction on the permanent displacements of wall facing. The peak ground acceleration had strong influence on the dynamic response of the walls. As an example, when the peak ground acceleration was 0.2g, 0.4g, and 0.6g permanent displacements for a wall with 9m height were 17cm, 28cm, and 32cm, respectively. It can be seen that peak ground acceleration and permanent displacements were correlated nonlinearly. Also the permanent displacement and L/H ratio correlation was nonlinear.

The study intended to use the ANN model in order to make reliable predictions for geosynthetic reinforced wall design and to check whether the results of finite element analysis results fall between reasonable limits.

The ANN was used to synthesize data derived from finite element studies on back to back geosynthetic reinforced retaining walls under seismic excitation. The input parameters used in the model were H, L, L/H,  $S_v$ , Ftype, PGA, PGV, EPA, AI, CAV, ASI, and VSI. The permanent displacement of the wall was chosen the only output.

The important point of the seismic evaluation of the seismic response of the back to back MSE retaining wall is the selection of ground motion intensity measure IM for different earthquakes. In this study due to constant frequency (3 Hz) value of harmonic motions with different PGAs (0.2g, 0.4g and 0.6g), intensity measures; PGV, EPA, CAV, ASI, and VSI are linearly correlated with PGA values but AI is not. Therefore any of these IMs is enough to approach high coefficients of correlated ANN model.

Using ANN regression analysis, the scatter of the predicted ANN displacements relative to the displacements obtained using the finite element method were assessed. The results produced high coefficients of correlation for training and testing data of 0.997 and 0.989, respectively. So, the agreement of the neural network predicted displacements and deformation classification with Finite Element Analyses results were encouraging by the means of correlation since the coefficient values of  $R=0.99$  for ANN regression analysis were achieved.

## References

- [1] Anastasopoulos I., T., Georgarakos, V., Georgiannou, V., Drosos, R., Kourkoulis, 2010, "Seismic performance of bar-mat reinforced-soil retaining wall: Shaking table testing versus numerical analysis with modified kinematic hardening constitutive model", *Soil Dynamics and Earthquake Engineering*, 10.1016/j.soildyn.2010.04.020 journal homepage: [www.elsevier.com/locate/soildyn](http://www.elsevier.com/locate/soildyn)
- [2] Basheer, I.A., 2002, "Stress-strain behavior of geomaterials in loading reversal simulated by time-delay neural networks", *Journal of Materials in Civil Engineering*, 14(3), 270-273.
- [3] Bathurst, R.J., Hatami, K., 1998, "Seismic response analysis of a geosynthetic-reinforced soil wall", *Geosynthetics International*, 5(1-2):127-166.
- [4] Benardos, A.G. and D.C., Kaliampakos, 2004, "Modeling TBM performance with artificial neural networks", *Tunneling and Underground Space Technology*, 19(6), 597-605.
- [5] Fausett, L.V. 1994, "Fundamentals neural networks: Architecture, algorithms, and applications", Prentice-Hall, Englewood Cliffs, New Jersey.
- [6] Goh, A.T.C., K.S., Wong and B.B., Broms, 1995, "Estimation of lateral wall movements in braced excavation using neural networks", *Canadian Geotechnical Journal*, 32, 1059-1064.
- [7] Guler, E., E.Cicek M., Hamderi, M.M., Demirkan, 2011, "Numerical analysis of reinforced soil walls with granular and cohesive backfills under cyclic loads", *Bull Earthquake Eng.* DOI 10.1007/s10518-011-9322-y
- [8] Haykin, S.S., 1999, *Neural networks: a comprehensive foundation*. Upper Saddle River, N.J., Prentice Hall.
- [9] Kim, D.H., D.J., Kim, et al., 1999, "The application of neural networks and statistical methods to process design in metal forming processes", *International Journal of Advanced Manufacturing Technology* 15(12): 886-894.
- [10] Kim, Y. and B., Kim, 2008, "Prediction of relative crest settlement of concrete-faced rockfill dams analyzed using an artificial neural network model", *Computers and Geotechnics*, 35(3), 313-322.
- [11] Kramer, S.L., 1996, *Geotechnical Earthquake Engineering*, Prentice Hall, New Jersey.
- [12] Kung, G.T., E.C., Hsiao, M., Schuster and C.H., Juang, 2007, "A neural network approach to estimating deflection of diaphragm walls caused by excavation in clays" *Computers and Geotechnics*, 34(5), 385-396.
- [13] Ling, H.I., Y., Mohri, D., Leshchinsky, C., Burke, K., Matsushima, H., Liu, 2005 "Large-scale shaking table tests on modular-block reinforced soil retaining walls", *J Geotech Geoenviron Eng ASCE* 131(4):465-476
- [14] Lu, Y. 2005, "Underground blast induced ground shock and its modeling using artificial neural network", *Computers and Geotechnics*, 32(3), 164-178.
- [15] Shang, J.Q., W., Ding, R.K., Rowe and L., Josic, 2004, "Detecting heavy metal contamination in soil using complex permittivity and artificial neural networks", *Canadian Geotechnical Journal*, 41(6), 1054-1067.
- [16] Uang, C.H. and V.V., Bertero, 1988, *Implications of recorded earthquake ground motions on seismic design of buildings structures*, UCB/EERC-88/13, California.
- [17] Ural, D.N. and H., Saka, 1998, "Liquefaction assessment by neural networks", *Electronic Journal of Geotechnical Engineering*, <http://www.ejge.com/Ppr9803/Ppr9803.htm>
- [18] Yoo, C. and J., Kim, 2007, "Tunneling performance prediction using an integrated GIS and neural network", *Computers and Geotechnics*, 34(1), 19-30.sa
- [19] Young-Su, K. and K., Byung-Tak, 2006, "Use of artificial neural networks in the prediction of liquefaction resistance of sands", *Journal of Geotechnical and Geoenvironmental Engineering*, 132(11), 1502-1504.
- [20] Zevgolis, I., 2007, "Numerical and Probabilistic Analysis of Reinforced Soil Structures", PhD Thesis, Purdue University.
- [21] Zhu, J.H., M.M., Zaman and S.A., Anderson, 1998a,



- “Modeling of soil behavior with a recurrent neural network”, Canadian Geotechnical Journal, 35(5), 858-872.
- [22] Zhu, J.H., M.M., Zaman and S.A., Anderson, 1998b, “Modeling of shearing behavior of a residual soil with recurrent neural network”, International Journal of Numerical and Analytical Methods in Geomechanics, 22(8), 671-687.
- [23] Zurada, J.M., 1992, Introduction to artificial neural systems, West Publishing Company, St. Paul.